

Preparation and characterization of di-hexadecanol maleic/triallyl isocyanurate crosslinked copolymer as solid-solid phase change materials

Xuelin Huang,¹ Jing Guo,^{1,2} Qingda An,¹ Xueyong Gong,^{1,2} Yumei Gong,^{1,2} Sen Zhang^{1,2}

¹School of Textile and Material Engineering, Dalian Polytechnic University, Dalian 116034, People's Republic of China

²Liaoning Engineering Technology Research Centre of Function Fiber and Its Composites, Dalian 116034,

People's Republic of China

Correspondence to: J. Guo (E-mail: guojing8161@163.com)

ABSTRACT: Di-hexadecanol maleic/Triallyl isocyanurate crosslinked copolymers as a novel solid–solid phase change materials were successfully synthesized through bulk polymerization. TAIC is the skeleton and DM is a functional side chain that stores and releases heat during its phase transition process. Fourier transform infrared spectroscopy, wide-angle X-ray diffraction, polarizing optical microscopy, differential scanning calorimetry, and thermogravimetry were employed to study the composition, chemical structure, crystalline properties, phase transition behaviors, and the thermal stability of the crosslinked copolymers, respectively. The test results indicate that DM/TAIC crosslinked copolymers have good thermal reliability and heat storage durability after 500 thermal cycles. The phase change temperatures of DM/TAIC crosslinked copolymers were approximately 28.24–37.02 °C, and it has high latent heat storage capacity of more than 83 J/g. At the same time, DM/TAIC crosslinked copolymers have good thermal stability, and they can be processed or used in high temperature environments. © 2016 Wiley Periodicals, Inc. *J. Appl. Polym. Sci.* **2016**, *133*, 44065.

KEYWORDS: copolymers; crosslinking; crystallization; differential scanning calorimetry (DSC); thermal properties

Received 26 April 2016; accepted 15 June 2016

DOI: 10.1002/app.44065

INTRODUCTION

Phase change material (PCM) is a kind of material that can change physical properties and provide latent heat with the temperature. The use of PCM's latent heat to control the absorption and release of energy can improve energy efficiency and alleviate the problem of energy shortage.^{1–5} Polymer-based solid–solid PCMs (SSPCMs) are characterized with high thermal energy storage, low coefficient of expansion and volume changes, no supercooling phenomena and phase separation, nontoxic, noncorrosive, nonpolluting, and stable performance, by changing conditions on the phase transition temperature control, it need not have special latent storage devices or containers to encapsulate the PCM, etc. Polymer-based SSPCM is a kind of new functional material with good prospects, and it is currently a hot spot in research.^{6–9}

To summarize, there are two basic methods to prepare polymer-based SSPCMs. One is the physical method based on the compatibility of polymer solid–liquid PCM with the carrier matrix, in which the two are fused together and made into a homogeneous PCM, so as to achieve the double purpose of high phase change enthalpy, and shape stability. Mu *et al.*¹⁰ prepared the

phase change fiber via electro spinning from the copolymer of poly(styrene-*co*-acrylonitrile) and lauric acid. The results indicate that the phase change fiber has suitable temperature, enthalpy of phase transition, and good ability to store thermal energy. Tang *et al.*¹¹ prepared the shape-stable phase change composite of fatty acid eutectics with diatomite by absorbing liquid fatty acid eutectics into diatomite, and added a small amount of graphite to improve the thermal conductivity of the PCM. The results showed that these composites have appropriate phase change temperature in the range of 18.2–28.7 °C, and it had high latent heat storage capacity of more than 100 J/g. The other is the chemical method in which PCMs are bound onto supporting polymeric materials by chemical grafting, blocking, and crosslinking copolymerization.¹² Moreover, after being bound onto supporting polymeric materials, PCMs will keep the macro shape in the process of phase change. At the same time, the adjustment of the phase change temperature and the enthalpy of phase change is realized by controlling the reaction conditions. Mu *et al.*¹² prepared a new SSPCMs by grafting PEG to the main chain of poly(styrene-*co*-acrylonitrile). Li *et al.*¹³ prepared the melamine/formaldehyde/polyethylene glycols (MFPEG) crosslinking copolymer SSPCM by amine-

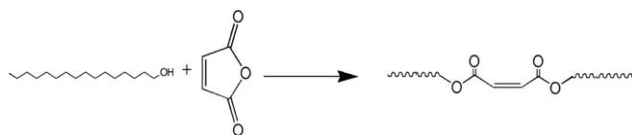


Figure 1. Synthesis process of DM.

aldehyde condensation reaction. The SSPCM has good performance and is useful for high-temperature thermal energy storage. Chen *et al.*¹⁴ prepared the poly(ethylene glycol) (PEG10000)/poly(glycidyl methacrylate) (PGMA) crosslinked copolymer as a novel SSPCM through the ring-opening crosslinking reaction of end-carboxyl groups in carboxyl poly(ethylene glycol) (CPEG) and epoxy groups in PGMA. The differential scanning calorimetry (DSC) results indicate that the copolymer imparts balanced and reversible phase change behaviors at the temperature range of 25–60 °C, and it has high latent heat storage capacity of more than 70 J/g. Thermogravimetric analysis (TGA) test showed that the decomposing temperature range of PGMA was about 380–420 °C in nitrogen atmosphere.

At present, SSPCMs are mainly based on poly(ethylene glycol) (PEG), methoxypoly(ethylene glycol)s, and fatty acid as functional PCMs, such as cellulose-*g*-PEG,¹⁵ P(AN-*co*-AM)-*g*-MAPEG,¹⁶ PEG/SiO₂,¹⁷ Poly(vinyl alcohol)-*g*-poly(ethylene glycol) monomethyl ether polymeric,¹⁸ multi fatty acid complex,^{19–21} etc. Among the studied PCMs, advanced fatty alcohol has been used as a latent heat energy storage material with the advantages of regular chain structure, good crystallinity, latent heat of phase change, and good chemical stability.^{22–24} But being prone to leakage in phase transition processes, fatty alcohol is easy to pollute the environment which limits the application of the PCMs. Liu *et al.*²⁵ prepared the SSPCMs by grafting the higher fatty alcohol onto poly(ethylene-maleic anhydride). The results indicated that the phase transition temperature of SSPCMs ranged from 36.4 °C to 67.1 °C, and the enthalpy of phase transformation of SSPCMs were from 125.7 to 146.2 J/g. Wang *et al.*²⁶ prepared the SSPCM by grafting the higher fatty alcohol onto poly(styrene-maleic anhydride). The phase transition temperature and the enthalpy of phase transformation of SSPCMs are 13.5–73.7 °C and 37.9–110.7 J/g, respectively.

Table I. The Mass Ratio of DM/TAIC Crosslinking Copolymers

| Sample | SSPCM-1 | SSPCM-2 | SSPCM-3 |
|---------------------------|---------|---------|---------|
| The mass ratio of DM/TAIC | 5:1 | 3:1 | 1:1 |

Di-hexadecanol maleic (DM)/Triallyl isocyanurate (TAIC) crosslinked copolymers as a novel SSPCMs were successfully synthesized through bulk polymerization. TAIC is the skeleton and DM is a functional side chain that stores and releases heat during its phase transition process. The chemical structure, crystalline properties, phase transition behaviors, and thermal stability of DM/TAIC crosslinking copolymers were investigated by FT-IR, polarizing optical microscopy (POM), Wide-angle X-ray diffraction (WAXD), DSC, and TGA, respectively. The results indicate that DM/TAIC crosslinked copolymers possess excellent phase change properties and an applicable temperature range, which could find the promising applications in solar energy storage and building.

EXPERIMENTAL

Materials

Hexadecanol (>98%, HD) and maleic anhydride (>99.5%, MA) were purchased from Chinese Medicine Group Chemical Reagent, and used without further purification. TAIC (>98%, TAIC) was purchased from Suzhou Chemical. Benzoyl peroxide (>99%, BPO) was purchased from Tianjin Fu Chen Chemical Reagents Factory.

Phase Transformation Monomer

Phase transformation monomer synthesis was conducted through adding MA, HD, and *p*-toluenesulfonic acid into a three-neck round-bottom flask with an over head stirrer at mass ratio 1:2.1:0.1. The temperature was set at a certain value varying from room temperature to 90 °C, later a precursor mixture was prepared by stirring gently for 3 h. After adding 50 mL water, the mixture of the precursor was put into a constant temperature oven at 90 °C. After static 5 min, the mixture was separated by a separatory funnel to remove the excess of the

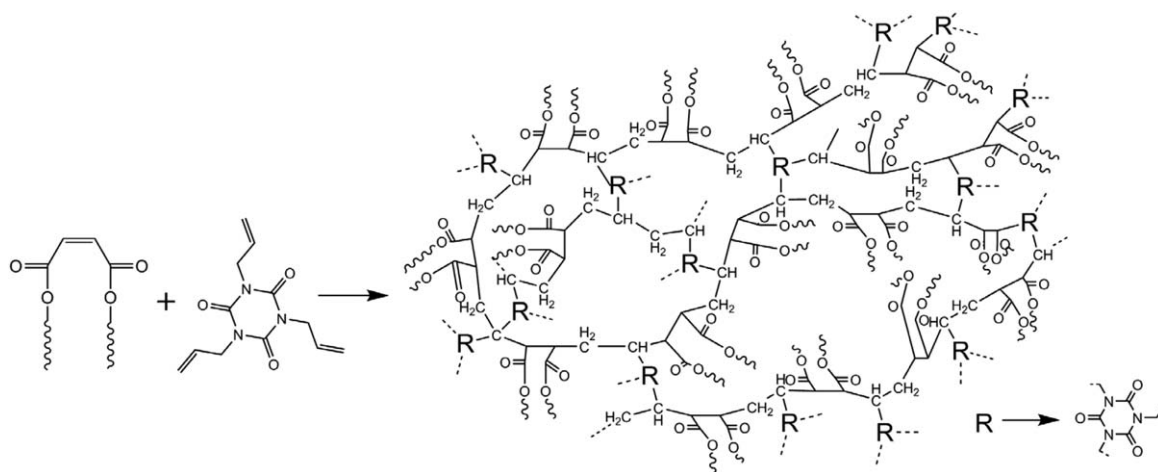


Figure 2. Synthesis process of DM/TAIC crosslinking copolymer.

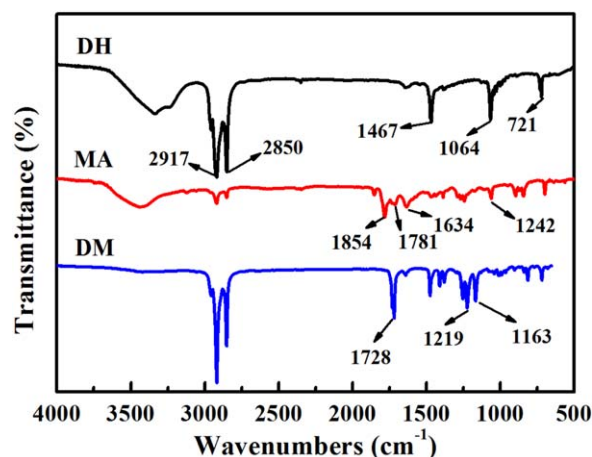


Figure 3. FT-IR spectra of DH, MA, and DM. [Color figure can be viewed in the online issue, which is available at wileyonlinelibrary.com.]

MA, and then dried at 30 °C to get DM. The reaction equation is shown in Figure 1.

DM/TAIC Crosslinked Copolymers SSPCMs

DM/TAIC crosslinked copolymers synthesis conducted through DM/TAIC, TAIC, and benzoyl peroxide (BPO) were added into three-neck round-bottom flask with an over head stirrer at mass ratio 1:*m*:*n* ($n = [m + 1]3\%$), with nitrogen as protective gas. The temperature was set at a certain value varying from room temperature to 110 °C. After 40 min reaction, crosslinked structure of DM/TAIC copolymer SSPCMs was obtained. The reaction equation is shown in Figure 2 and the ratio of DM and TAIC is list in Table I.

Characterization

Fourier Transform Infrared Spectroscopy. Fourier transform infrared spectroscopy (FT-IR) spectra of DH, MA, DM, TAIC, and DM/TAIC crosslinked copolymers were taken by a Spec-teum One-B Infrared Spectrophotometer. The samples were mixed with KBr and then pressed into a pellet. Wavenumber test range was from 4000 to 400 cm^{-1} .

Wide-Angle X-ray Diffraction. WAXD patterns of the DM and DM/TAIC crosslinked copolymers were recorded on D/Max-3b at a condition of 30 mA and 40 kV. The X-ray source is an 18

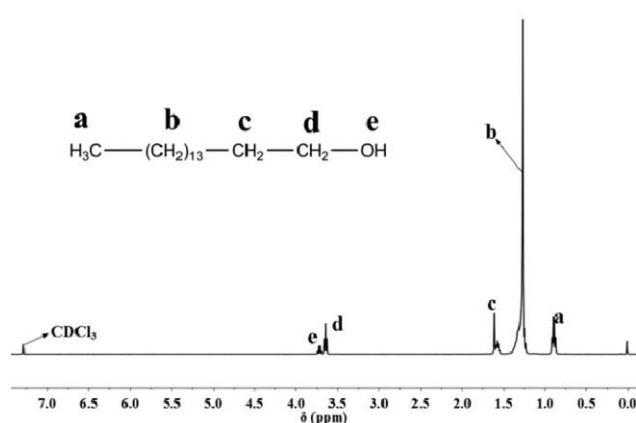


Figure 4. $^1\text{H-NMR}$ spectrum of DH.

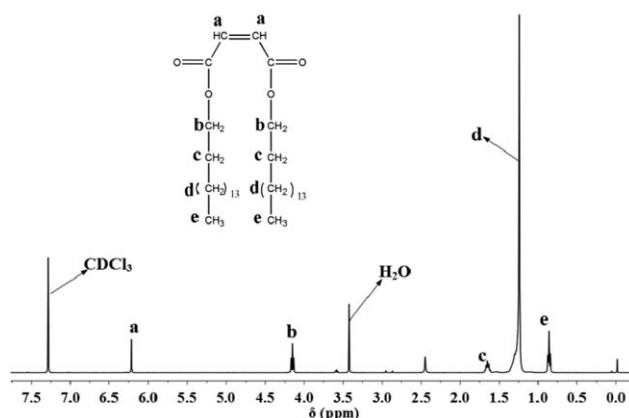


Figure 5. $^1\text{H-NMR}$ spectrum of DM.

kW rotating anode X-ray generator equipped with a Cu target. Measurements were collected from $2\theta = 10^\circ$ to 45° .

Polarized Optical Microscopy. The crystallization and melting behavior of the material was observed by DE EP200 hot stage polarizing (POM). The measurements were performed at a temperature range of 0–100 °C.

Thermal Property Investigation. The thermal properties of the DM and DM/TAIC crosslinked copolymers were performed with a DSC Q2000 under nitrogen gas. Temperature and enthalpy were calibrated with an indium standard. The samples (5–10.0 mg) were heated to 100 °C and held at this temperature for 2 min to erase the thermal history, followed by cooling to 0 °C and then heated to 100 °C at the heating rate of 10 °C/min. The second running was used to analyze thermal behavior.

Thermogravimetry. Thermogravimetric analysis (TGA) was performed using a Q600 (TA Instruments, New Castle, Delaware, USA) from room temperature to 700 °C with a heating rate of 10 °C/min under nitrogen atmosphere.

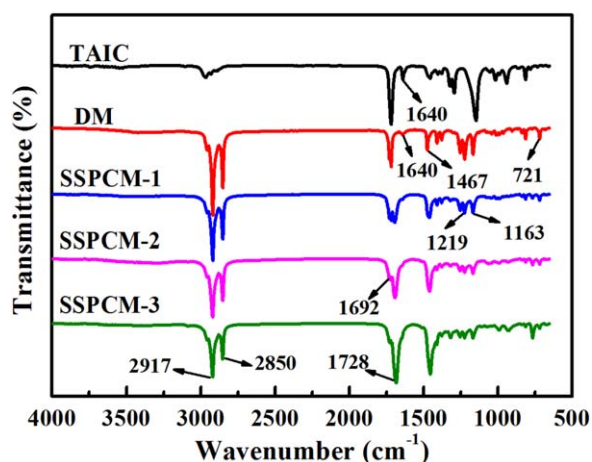


Figure 6. FT-IR spectra of TAIC, DM, SSPCM-1, SSPCM-2, and SSPCM-3. [Color figure can be viewed in the online issue, which is available at wileyonlinelibrary.com.]

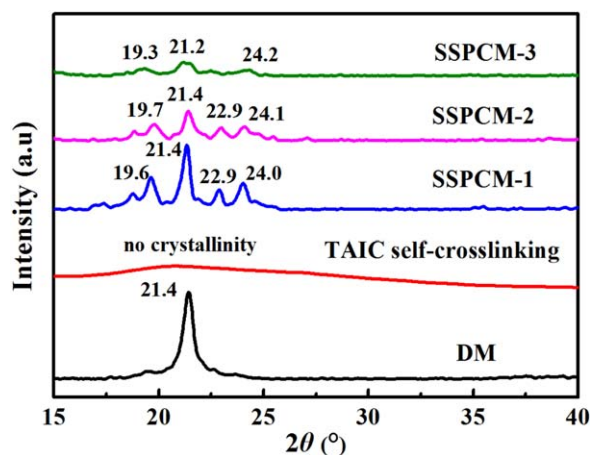


Figure 7. XRD spectra of DM, TAIC self-crosslinking, SSPCM-1, SSPCM-2, and SSPCM-3. [Color figure can be viewed in the online issue, which is available at wileyonlinelibrary.com.]

RESULTS AND DISCUSSION

Chemical Characterization of DM and DM/TAIC Crosslinked Copolymers

Figure 3 shows the FT-IR spectra of DH, MA, and DM. The absorption bands at 2917, 2850, 1467, and 721 cm^{-1} represent the characteristic of DH molecular structure. The characteristic bands of MA appear at 1854, 1781, 1634, and 1242 cm^{-1} . For DM phase change monomer, the absorption peaks of C=O and

C=O in DM appear at 1219, 1163, and 1728 cm^{-1} , respectively. They have verified the existence of ester groups, i.e. proof of products containing aliphatic polyester syndrome group. These results proved that DM had been successfully fabricated.

The $^1\text{H-NMR}$ spectrum of DH is shown in Figure 4. The peak at $\delta = 3.76\text{--}3.69$ ppm is the proton signals of the -OH. Figure 5 shows the $^1\text{H-NMR}$ spectrum of DM. The peak at $\delta = 6.18\text{--}6.25$ ppm is the proton signals of the --CH=CH-- , and the peak at $\delta = 4.11\text{--}4.19$ ppm is the proton signals of the $\text{--O--CH}_2\text{--}$. The appearance of peaks at $\delta = 6.18\text{--}6.25$ ppm and 4.11–4.19 ppm, and the disappearance of peaks at $\delta = 3.76\text{--}3.69$ ppm indicate that DM was synthesized successfully.

Figure 6 shows the FT-IR spectra of TAIC, DM, and DM/TAIC crosslinked copolymers. For DM/TAIC crosslinked copolymers, the absorption peaks at 1410 cm^{-1} are attributed to the stretching vibration of C–N, and 1728 and 1692 cm^{-1} are the characteristic absorption peaks of C=O in ester and ketone groups. With the increase of TAIC, the absorption peak of 1728 cm^{-1} gradually disappeared. The reason for this phenomenon may be that the absorption peak of ketone group is close to the base of the ester group, and the content of the ketone group is higher than ester group, so it only shows the characteristic absorption peak of ketone groups. The absorption peak disappeared at 1640 cm^{-1} , proving that DM/TAIC crosslinked copolymers had been successfully fabricated, and the reaction had been completed.

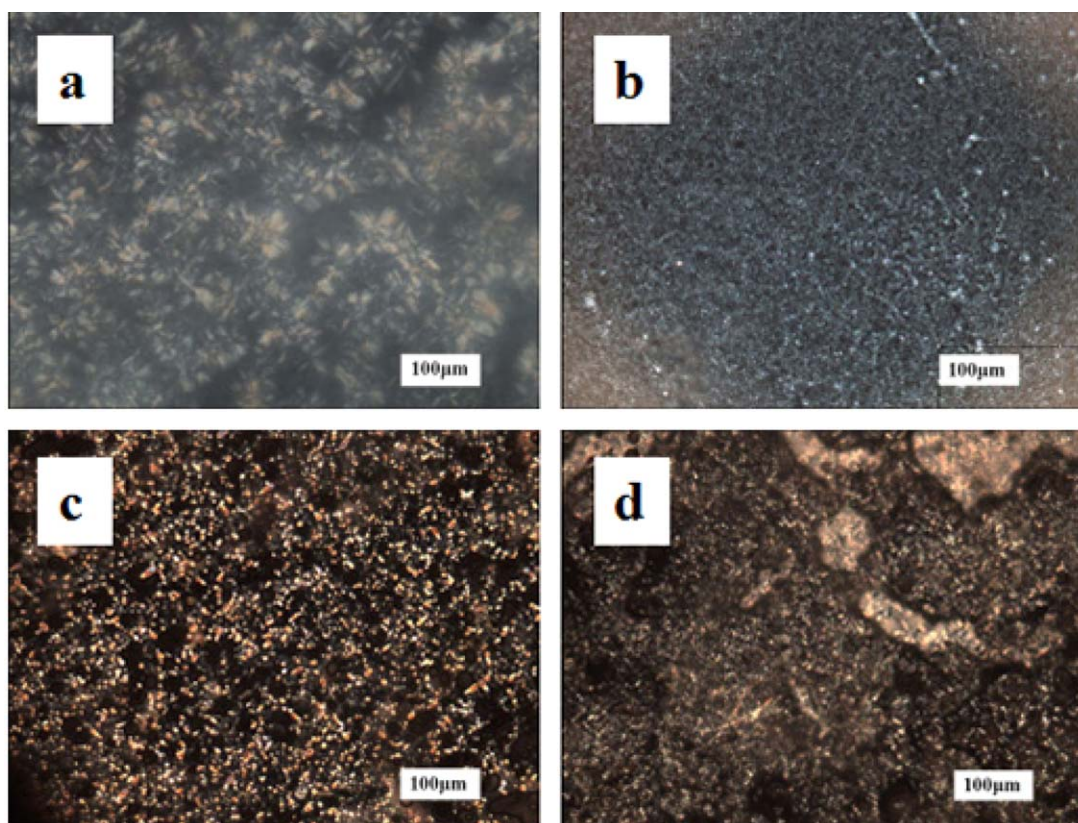


Figure 8. POM of (a) DM, (b) SSPCM-1, (c) SSPCM-2, and (d) SSPCM-3. [Color figure can be viewed in the online issue, which is available at wileyonlinelibrary.com.]

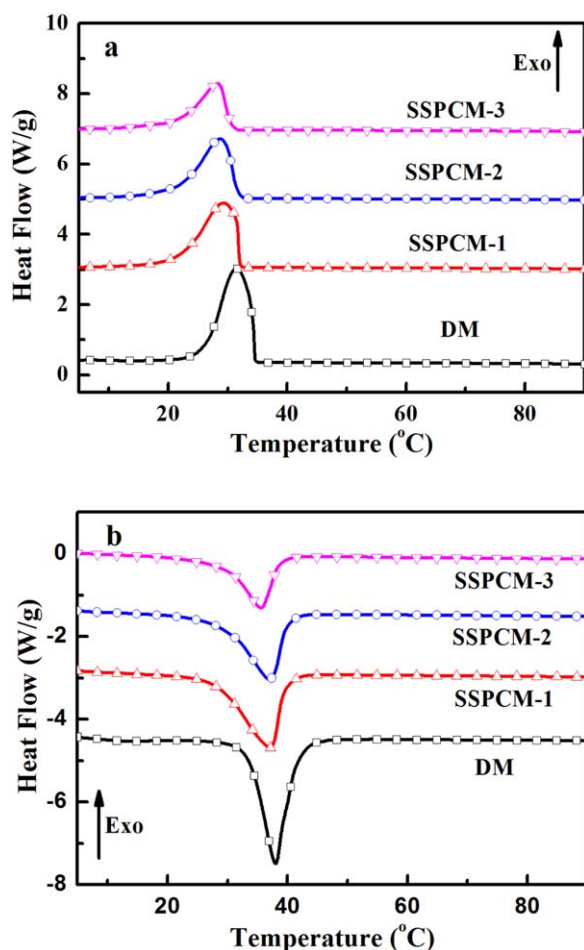


Figure 9. DSC curves of DM, SSPCM-1, SSPCM-2, and SSPCM-3 in the cooling [Figure 7(a)] and heating [Figure 7(b)] process. [Color figure can be viewed in the online issue, which is available at wileyonlinelibrary.com.]

Crystallization Properties of DM/TAIC Copolymer

To reveal the crystalline properties of the synthesized SSPCMs, the XRD patterns at room temperature of DM and DM/TAIC crosslinked copolymers are shown in Figure 7. As a comparison, WXR pattern of TAIC self-crosslinked copolymer is displayed in Figure 7 too. It is not difficult to find that DM and DM/TAIC have sharp diffraction peaks at different diffraction angles, which indicates that they show crystallinity. There is a main diffraction peak at about 21.4° in the XRD curve of DM and DM/TAIC. Apparently, the diffraction peaks of DM/TAIC crosslinked copolymers are lower and wider than that of DM.

There are a series of new diffraction peaks at about 19.7° , 22.9° , 24.1° as shown in the XRD curve. The results indicate that DM/TAIC copolymer changed the molecular structure, which led to the loss of crystallinity. At the same time, with the increase of TAIC, the intensity of the diffraction peaks decreased obviously, which is possibly ascribed to the low crystallization ability of the restricted alkyl side groups onto copolymer backbones.^{24,26} In addition, with the increase of TAIC, the minor peak-shift for DM/TAIC crosslinked copolymers. The detailed crystal structures and its packing manner of confined alkyl side groups need to be further investigated in the future.

In order to further reveal the crystalline properties of DM/TAIC crosslinked copolymers, the POM was used to record the crystallinity of DM and DM/TAIC. It is observed from Figure 8 that both DM and DM/TAIC are crystalline. However, under the same test condition, the crystallite size of DM/TAIC are much smaller than DM, which indicates that the crystalline structure of DH segment in DM/TAIC has been destroyed to some extent by the crosslinked structure of SSPCM. These results are in good agreement with XRD results.

Thermophysical Properties of DM/TAIC Crosslinked Copolymers

Phase Change Properties of DM/TAIC Crosslinked Copolymers

To investigate the phase change properties of the synthesized PCM, the DSC analysis is a necessary measurement. Figure 9 shows the DSC of DM and DM/TAIC crosslinked copolymers, the phase change temperature and enthalpy of DM and DM/TAIC crosslinked copolymers with different TAIC ratios are listed in Table II. For DM phase change monomer, T_m , T_c , and heat enthalpy (ΔH_m) peak at 38.03°C , 31.44°C , and 105.2 J/g , respectively. The same shifting regular pattern is obviously presented in Figure 9 and Table II, both phase transition temperature and latent enthalpy decrease with the increase of TAIC content. There may be two reasons for this phenomenon. The first reason is that the TAIC has good stability in the process of DM crystallization, and it is not contributing to the enthalpy of phase transformation. Secondly, TAIC is an impurity in the process of DM crystallization, and it will destroy the regularity of the crystalline region, so that the degree of crystallinity is decreased. Therefore, it leads to the decrease of the phase transition temperature and the enthalpy of phase change. Thirdly, in the DM/TAIC crosslinked copolymers network, DM molecular chains is confined by TAIC skeleton, consequently the arrangement and orientation of DM molecules are suppressed and restricted partially by the steric effect, which results in the reduction of the crystalline

Table II. The DSC Parameters of DM, SSPCM-1, SSPCM-2, and SSPCM-3

| Sample | T_c ($^\circ\text{C}$) | ΔH_c (J/g) | Theoretical value (%) | T_m ($^\circ\text{C}$) | ΔH_m (J/g) | Theoretical value (%) | Phase behavior |
|---------|----------------------------|--------------------|-----------------------|----------------------------|--------------------|-----------------------|----------------|
| DM | 31.44 | 103.10 | — | 38.03 | 105.2 | — | Solid—liquid |
| SSPCM-1 | 29.25 | 82.42 | 95.93 | 37.02 | 83.01 | 94.69 | Solid—solid |
| SSPCM-2 | 28.63 | 72.41 | 93.64 | 37.01 | 73.12 | 92.67 | Solid—solid |
| SSPCM-3 | 28.24 | 46.97 | 91.12 | 35.61 | 47.12 | 89.58 | Solid—solid |

Table III. Thermal Energy Storage Characteristics of Different Shape Stabilized PCMs in Literatures

| Sample | T_c (°C) | T_m (°C) | Theoretical enthalpy (J/g) | Latent heat (J/g) | Enthalpy efficiency (%) | Reference |
|-------------------------------|------------|------------|----------------------------|-------------------|-------------------------|-----------|
| PEG8000/PLA (66.67 wt %) | 43.6 | 63.7 | 111.87 | 74.7 | 66.77 | 30 |
| PEG10000/PGMA (85 wt %) | 39.2 | 63.4 | 141.7 | 73.2 | 51.66 | 14 |
| PEG4000/MDI/PVA (79.65 wt %) | 34.2 | 61.1 | 134.13 | 72.8 | 54.28 | 28 |
| PEG8000/cellulose (60 wt %) | 37.05 | 58.51 | 125.14 | 84.63 | 67.28 | 31 |
| PEG8000/agarose (70 wt %) | 43.36 | 57.73 | 146 | 110.86 | 75.93 | 31 |
| PEG8000/chitosan (80 wt %) | 44.76 | 57.18 | 166.86 | 152.16 | 91.19 | 31 |
| P(AN-co-IA)/PEG4000 (73 wt %) | 35.55 | 53.9 | 134.9 | 118.56 | 87.89 | 32 |
| SMA/PEG10000 (80 wt %) | 41.9 | 59.8 | 161.84 | 128.9 | 79.65 | 33 |
| PAN/MAPEG (50 wt %) | 16.27 | 51.45 | 83.17 | 74.16 | 89.17 | 34 |
| SSPCM-1 | 29.25 | 37.02 | 87.67 | 83.01 | 94.69 | Present |
| SSPCM-2 | 28.63 | 37.01 | 78.9 | 73.12 | 92.67 | Present |
| SSPCM-3 | 28.24 | 35.61 | 52.6 | 47.12 | 89.58 | Present |

segments and the decrease of the crystalline regions. Therefore, the phase transition performances of the copolymer decline for the crosslinked structure.^{13,27–29}

In addition, Table III shows the comparison of energy storage properties of SSPCM1-3 with that of other SSPCMs in literatures Refs. 14, 28, 30–34. In which the enthalpy efficiency (ψ) is

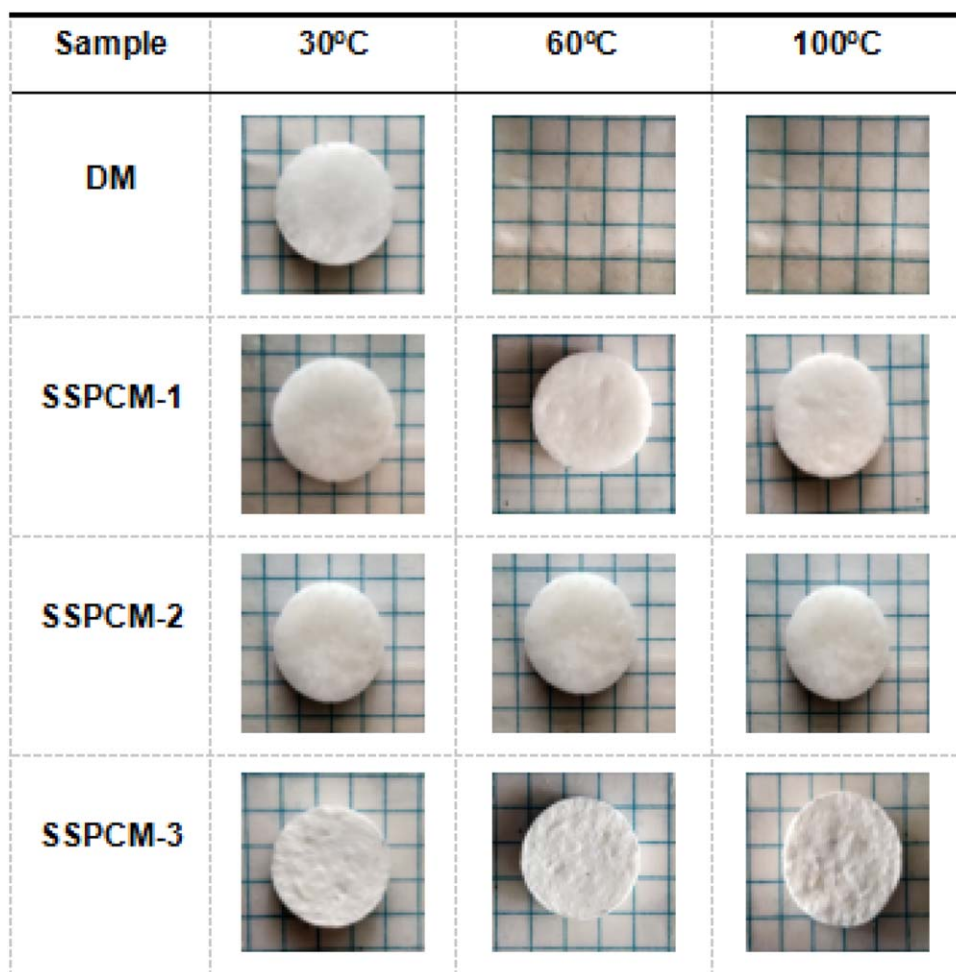


Figure 10. Compared thermal shape stability of DM, SSPCM-1, SSPCM-2, and SSPCM-3 with temperature. [Color figure can be viewed in the online issue, which is available at www.wileyonlinelibrary.com.]

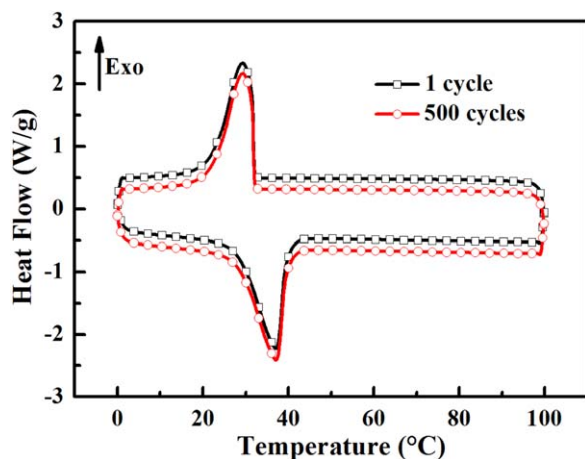


Figure 11. DSC curves of SSPCM-1 after the different thermal cycling treatment. [Color figure can be viewed in the online issue, which is available at wileyonlinelibrary.com.]

defined as the ratio of practical and theoretical loading in mixtures. By considering these data it is appreciably noted that the ψ value of SSPCMs in present work are much higher than other SSPCMs in literatures.

Shape-Stability Properties of DM/TAIC Crosslinked Copolymers. Figure 10 gives the compared shape stability of DM and DM/TAIC crosslinked copolymers. Under the same scale, DM and DM/TAIC show the different thermal shape stability with temperature changing from 30 °C to 100 °C. As seen from Figure 10, while being heated to 60 °C above the phase change temperature of DM, DM changes into liquid. However, even if the temperature rises to 100 °C, DM/TAIC still kept in shape perfectly and have no liquid leakage on the surface. The results showed that DM/TAIC crosslinked copolymers are shape stable, and the absence of liquid leakage reveals their effective utilization in building and clothing applications.

Thermal Reliability of DM/TAIC Crosslinked Copolymer. To verify the stability of phase change for SSPCM-1, the 1 and 500 thermal cycles were carried out by DSC, as shown in Figure 11. Thermal data from DSC are summarized in Table IV, the phase transition temperatures and latent heat values of the SSPCM-1 slightly alter after 500 cycles. These results indicate that DM/TAIC crosslinked copolymers have good energy storage, release effect, and great application prospects.

Thermal Stability of DM/TAIC Crosslinked Copolymers. TGA curves are shown in Figure 12(a) to determine thermal stability of pure components and composites. Differential thermal gravity (DTG) [Figure 12(b)] is performed to determine the maximum rate of weight loss of the composites, and the

Table IV. DSC Data of SSPCM-1 under Different Thermal Cycles

| Sample | T_c (°C) | ΔH_c (J/g) | T_m (°C) | ΔH_m (J/g) | Phase behavior |
|------------|------------|--------------------|------------|--------------------|----------------|
| 1 cycle | 29.25 | 82.42 | 37.02 | 83.01 | Solid-solid |
| 500 cycles | 29.23 | 81.66 | 37.00 | 82.32 | Solid-solid |

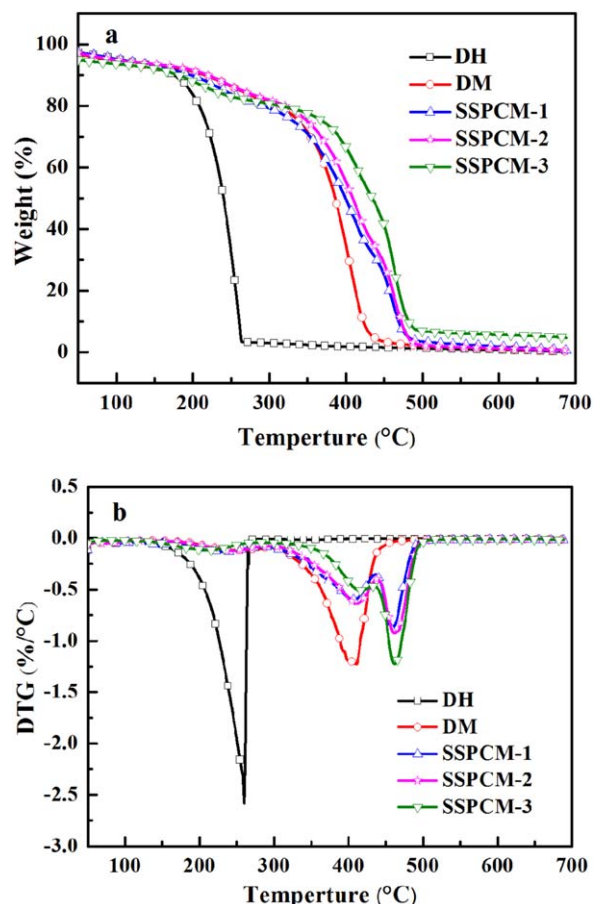


Figure 12. (a) TGA and (b) DTG spectra of DH, DM, SSPCM-1, SSPCM-2, and SSPCM-3. [Color figure can be viewed in the online issue, which is available at wileyonlinelibrary.com.]

results are summarized in Table V. DH mainly has a decomposition interval from 160 °C to 260 °C, and the maximum value is reached at 260 °C. The degradation of DM occurred mainly in 310–465 °C, and the maximum thermal decomposition rate reached a maximum at 410 °C. DM/TAIC crosslinked copolymers displayed three-step thermal degradation process as compared with DH. The first degradation occurred between 160 °C and 268 °C, which is contributed from a small amount of monomer in DH. After that, DM/TAIC crosslinked copolymers presents the second decomposition process originated from the grafted DH-alkyl side groups with further temperature

Table V. Characteristics Temperatures of TGA and DTG Curves of DH, DM, SSPCM-1, SSPCM-2, and SSPCM-3

| Sample | T_{max1} (°C) | T_{max2} (°C) | $T_{50\%}$ | Char yield at 700 °C (wt %) |
|---------|-----------------|-----------------|------------|-----------------------------|
| DH | 260 | - | 240 | 4.8 |
| DM | 410 | - | 386 | 2.1 |
| SSPCM-1 | 412 | 460 | 399 | 1.1 |
| SSPCM-2 | 411 | 461 | 409 | 0.3 |
| SSPCM-3 | 413 | 461 | 435 | 0.1 |

increasing. With further temperature increasing, DM/TAIC crosslinked copolymers presents the third decomposition process contributed from SSPCMs backbones. DM/TAIC crosslinked copolymers and DM in contrast, DM/TAIC crosslinked copolymers degradation temperature have a slight increase. It is because of the crosslinked network played a very important role in elevating the thermal resistance of DM/TAIC crosslinked copolymers. Thus, the synthesized novel DM/TAIC crosslinked copolymers with good heat-resistant performance will have a broad applicable temperature range.

CONCLUSIONS

A new type of novel DM/TAIC crosslinked copolymers were successfully synthesized via a two-step chemistry reaction, and the SSPCMs still kept solid state even if the temperature is raised to 100 °C or higher because the TAIC skeleton and the crosslinked structure restricts the free movement of DM molecular chains at high temperature. The results show that the synthesized DM/TAIC crosslinked copolymers have excellent phase change properties with a suitable solid–solid phase transition temperature range of 28.24–37.02 °C and a high latent enthalpy within the range of 46.97–83.01 J/g. Furthermore, DM/TAIC crosslinked copolymer display the better thermal stability, which can be used as shape-stabilized PCMs for thermal energy storage.

ACKNOWLEDGMENTS

Supported by National Natural Science Foundation of China (No. 51373027) and Liaoning Science and Technology Foundation of China (No. 2015020221).

REFERENCES

1. Pielichowska, K.; Pielichowski, K. *Prog. Mater. Sci.* **2014**, *65*, 67.
2. Sari, A.; Biçer, A. *Energy Build.* **2012**, *51*, 73.
3. Zhang, N.; Yuan, Y.; Yuan, Y.; Li, T.; Cao, X. *Energy Build.* **2014**, *82*, 505.
4. Cai, Y.; Sun, G.; Liu, M.; Zhang, J.; Wang, Q.; Wei, Q. *Sol. Energy* **2015**, *118*, 87.
5. Sari, A.; Alkan, C.; Karaipekli, A.; Uzun, O. *Appl. Polym. Sci.* **2009**, *116*, 929.
6. Chen, C.; Liu, W.; Wang, H.; Peng, K. *Appl. Energy* **2015**, *152*, 198.
7. Cai, Y.; Xu, X.; Gao, C.; Bian, T.; Qiao, H.; Wei, Q. *Mater. Lett.* **2012**, *89*, 43.
8. Mei, D.; Zhang, B.; Liu, R.; Zhang, Y.; Liu, J. *Int. J. Energy Res.* **2011**, *35*, 828.
9. Wang, Y.; Xia, T.; Zheng, H.; Feng, H. *Energy Build.* **2011**, *43*, 2365.
10. Mu, S.; Guo, J.; Zhang, B.; Qi, S.; Yang, L.; Wang, D. *Macromol. Sci. A* **2015**, *52*, 699.
11. Tang, F.; Su, D.; Tang, Y.; Fang, G. *Sol. Energy Mater. Sol. Cells* **2015**, *41*, 218.
12. Mu, S.; Guo, J.; Gong, Y.; Zhang, S.; Yu, Y. *Chin. Chem. Lett.* **2015**, *26*, 1364.
13. Li, Y.; Wang, S.; Liu, H.; Meng, F.; Ma, H.; Zheng, W. *Sol. Energy Mater. Sol. Cells* **2014**, *127*, 92.
14. Chen, C.; Liu, W.; Yang, H.; Zhao, Y.; Liu, S. *Sol. Energy* **2015**, *85*, 2679.
15. Li, Y.; Liu, R.; Huang, Y. *Appl. Polym. Sci.* **2008**, *110*, 1797.
16. Şentürk, S.; Kahraman, D.; Alkan, C.; Gökçe, I. *Carbohydr. Polym.* **2011**, *84*, 141.
17. Zhang, L.; Guo, J.; Liu, Y.; Yang, L.; Zhang, B. *High Perform. Polym.* **2015**, *11*, 1.
18. Qian, T.; Li, J.; Ma, H.; Yang, J. *Sol. Energy Mater. Sol. Cells* **2015**, *132*, 29.
19. Zhang, M.; Ma, R.; Jiang, Z. *Chem. Res. Chin. U* **2004**, *10*, 1966.
20. Cellat, K.; Beyhan, B.; Güngör, C.; Konuklu, Y.; Karahan, O.; Dündar, C. *Energy Build.* **2015**, *106*, 156.
21. Wi, S.; Seo, J.; Jeong, S.; Chang, S.; Kang, Y.; Kim, S. *Sol. Energy Mater. Sol. Cells* **2015**, *143*, 168.
22. Sharma, A.; Shukla, A. *Energy Build.* **2015**, *99*, 196.
23. Aydin, A.; Aydin, A. *Sol. Energy Mater. Sol. Cells* **2012**, *96*, 93.
24. Tang, B.; Wang, L.; Xu, Y.; Xiu, J.; Zhang, S. *Sol. Energy Mater. Sol. Cells* **2016**, *144*, 1.
25. Shi, H.; Li, J.; Jin, Y.; Yin, Y.; Zhang, X. *Mater. Chem. Phys.* **2011**, *131*, 108.
26. Wang, H.; Shi, H.; Miao, Q.; Zhang, L.; Zhang, X.; Lu, Q. *Thermochim. Acta* **2013**, *564*, 34.
27. Liu, L.; Wang, H.; Qi, X.; Kong, L.; Cui, J.; Zhang, X.; Shi, H. *Cells* **2015**, *143*, 21.
28. Zhou, X. *J. Appl. Polym. Sci.* **2009**, *113*, 2041.
29. Li, W.; Ding, E. *Sol. Energy Mater. Sol. Cells* **2007**, *91*, 764.
30. Chen, C.; Liu, K.; Wang, H.; Liu, W.; Zhang, H. *Sol. Energy Mater. Sol. Cells* **2013**, *117*, 372.
31. Alkan, C.; Günther, E.; Hiebler, S.; Ensari, O.; Kahraman, D. *Sol. Energy* **2012**, *86*, 1761.
32. Mu, S.; Guo, J.; Yu, Y.; An, Q.; Zhang, S.; Wang, D. *Energy Convers. Manag.* **2016**, *110*, 176.
33. Tang, B.; Yang, Z.; Zhang, S. *Adv. Mater. Res.* **2012**, *557-559*, 1192.
34. Guo, J.; Xie, P.; Zhang, X.; Yu, C.; Guan, F.; Liu, Y. *J. Appl. Polym. Sci.* **2014**, *131*, DOI: 10.1002/app.40152.